The Eel Retina

Ganglion Cell Classes and Spatial Mechanisms

ROBERT M. SHAPLEY and JAMES GORDON

From The Rockefeller University, and Hunter College of the City University of New York, New York 10021, and the Marine Biological Laboratory, Woods Hole, Massachusetts 02543. Dr. Gordon's present address is Hunter College of the City University of New York, New York 10021.

ABSTRACT We have been able to separate optic fibers in the eye of the eel *Anguilla rostrata* into two distinct classes on the basis of spatial summation properties. X fibers, the first class, are like X ganglion cells in the cat: they have null positions for contrast reversal sine gratings; they respond at the modulation frequency; and many have a strong surround mechanism. $\bar{X}$ fibers, the second class, respond with an "*on-off*" response to local stimulation, to diffuse light modulation, to coarse drifting gratings, and to contrast reversal gratings. We have put forward a model for the receptive field of $\bar{X}$ fibers which involves two subunits, with rectification before the subunits add their signals. This model accounts for many of the quirks of $\bar{X}$ fibers.

INTRODUCTION

The neural activity of optic nerve fibers constitutes the output of the retina. Therefore, if one measures this activity when the retina is subjected to various visual patterns, one may be able to infer the neural transformations performed on the visual image by the retina. This general strategy has been used by many different investigators in a wide variety of vertebrate retinas (see Rodieck, 1973). Such an approach is complicated by the diversity of retinal ganglion cells in every vertebrate retina which has been studied (e.g., Hartline, 1938; Kuffler, 1953; Maturana, et al., 1960; Enroth-Cugell and Robson, 1966; Levick, 1967). Not only are there "*on*"-center, and "*off*"-center cells, but different ganglion cells seem to be connected to functionally different pathways within the retina. This is deduced from among other things the differing spatial summation properties, linear (X) or nonlinear (Y), characteristic of different classes of retinal ganglion cells (Enroth-Cugell and Robson, 1966). Recent work reinforces the concept of differential retinal wiring to distinct types of ganglion cell (Hochstein and Shapley, 1976*a*, *b*). Hochstein and Shapley demonstrated that Y cells were apparently excited by a dispersed ensemble of small neural nonlinear subunits which did not drive X cells in any significant way. The research on X and Y cells has been done mainly in the retina of the cat. There has been some related work in other mammalian retinas. Up to now it has been an open question to what extent these receptive field concepts apply to other classes of vertebrates.

In this paper, we extend the analysis of the spatial properties of retinal ganglion cells to the ganglion cells of a teleost fish, the eel *Anguilla rostrata*. We used the eel for the reasons mentioned in the previous paper: its physiological robustness; the relatively small number of nerve fibers in the eel optic nerve; and the possibility of extending this work in the future to the hormonally transformed eye of the migrating eel. We found many retinal ganglion cells in the eel retina which correspond to the X cells of the cat retina. They summed neural signals in a linear manner. Other ganglion cells in the eel retina exhibited nonlinearities either before or at the stage of spatial summation. We called these cells $\bar{X}$ cells, because they were not in the same category as X cells, yet they were unlike the Y-type retinal ganglion cells of the cat. In several respects these $\bar{X}$ cells resembled the *on-off* W cells in the cat retina (Stone and Fukuda, 1974; Cleland and Levick, 1974). Many of the $\bar{X}$ cells were locally *on-off* (Hartline, 1938). On the basis of the responses of these cells to a variety of visual patterns, we were able to devise a plausible model for the origin of the *on-off* response. This model for *on-off* retinal ganglion cells in the eel may be a first step in understanding the retinal interactions which lead to *on-off* responses in many vertebrate retinas.

MATERIALS AND METHODS

Biological Preparation

All the experiments described here were done on eyecups excised from the eel. The eel was dark adapted and decapitated, and then the eye was dissected and opened in dim red light. Moist oxygen was blown on the retina. The retina remained viable for up to 4 h.

Recordings

Nerve impulses were recorded extracellularly by a relatively blunt-tipped (2 μm tip diameter) micropipette which was advanced into one of the optic nerve fiber bundles on the surface of the retina. The electrode was advanced by means of a Kopf hydraulic drive with a stepping motor (David Kopf Instruments, Tujunga, Calif.). Amplified nerve impulses were led to an oscilloscope, an audio monitor, and a discriminator. The discriminator output was a 0.5-ms pulse. This pulse was fed into the microcomputer stimulator-averager described below. The discriminator pulse was also used to brighten the oscilloscope trace at the instant of triggering in order to provide a visual marker of the triggering level.

Visual Stimulator and Response Averaging

The visual stimulus was an intensity-modulated raster of lines on an oscilloscope screen (Tektronix 5103N without an internal graticule, P31 phosphor, Tektronix, Inc., Beaverton, Ore.). The oscilloscope screen was imaged on the eel retina with a lens and a mirror. The magnification of this system was 2:1, object:image. The size of the spatial pattern on the oscilloscope screen was 2.8 cm^2 and the mean unattenuated retinal illuminance of the oscilloscope screen was 2 lm/m^2. The mean retinal illuminance was reduced to 0.2 lm/m^2 by means of an Inconel ND 1.0 log filter. This was probably a high scotopic background for the eel ganglion cells. As was mentioned in the preceding paper, a monochromatic 520-nm background of roughly similar retinal illuminance

(0.066 $\mu W/cm^2 \equiv 0.44$ lm/m^2) was required to reveal a cone contribution to ERG responses. The broad-band P31 phosphor would tend to suppress the long-wavelength cones more than the 520-nm background.

We used a novel electronic instrument to control the visual stimulus and to average the neural responses. The visual stimulator-averager was designed as a special purpose microcomputer by Norman Milkman and David Kocsis and built in The Rockefeller University Electronics Shop. A more refined instrument of the same type has recently been built and is described by Milkman et al. (1977). The basic idea behind the visual stimulator averager was the use of a microprocessor as an organizer which could coordinate and control logical and analog circuits responsible for production of the electronic visual stimulus. Some of the signals under the microprocessor's control included the spatial waveform signal, the temporal modulation signal, the spatial offset, and the orientation angle of the pattern. The pattern was presented repetitively at a frame rate of 256 Hz and a line rate of 192 kHz. The circuitry for the spatial waveform was designed so that spatial frequency (cycles/millimeter) and temporal rate of drift (hertz) were independent variables. This allowed us to measure, for example, the spatial frequency response of a cell to drifting gratings all presented at a constant drift rate in hertz. Aperiodic spatial stimuli, bars and edges, were presented via a pulse generator which was synchronized to the frame rate (Shapley and Rossetto, 1976). Position, width, and direction of contrast were determined by the experimenter.

Spatial and temporal signals were multiplied in an analog multiplier in order to produce temporal modulation. In many experiments a contrast reversal (also called alternating phase) sine grating was used as a stimulus. This was produced by multiplying a slow sine modulation signal with a faster sine spatial waveform. The sine grating was stationary from frame to frame of the raster, but its position relative to the start of the sweep or, in other words, its spatial phase, was under program control. The depth of modulation for the temporally modulated bars or edges, and also for the contrast reversal grating, were also under the experimenter's control. The electronic visual stimulator also contained a rotator circuit (Shapley and Rossetto, 1976) which allowed us to measure any departure from radial symmetry of the receptive fields.

The contrast of a grating on the retina may be defined as $\frac{I_{max} - I_{min}}{2\, I_{mean}}$ where I_{max} is the peak retinal illuminance of the grating and I_{min} is the illuminance at the trough of the sine wave. As stated above, I_{mean} was 0.2 lm/m^2 and it was maintained at this level throughout the duration of the experiments. For contrast reversal gratings we will call the peak contrast the contrast. That is, we will say that the contrast of a contrast reversal grating is 0.1 if the grating reaches a contrast of 0.1 when the temporal modulation signal is at its peak. The contrast for a modulated bar or edge follows the same convention. The contrast on the oscilloscope screen was linear with modulation depth up to 0.5 contrast, and all our measurements were in this range.

The neural response was measured by averaging nerve impulses in bins which were phased to the stimulus cycle. The duration of the experimental run was typically 15 s although it was 30 s for the slower temporal modulation signals (<1 cps) which were occasionally used. Averaged response histograms were read out from the microcomputer memory through a digital-to-analog converter onto a chart recorder. Precise measurements of peak heights and Fourier coefficients in the response were made possible by digitizing the chart recorder records with a Grafpen tablet and the Fourier-analyzing the digitized averaged response (cf. Hochstein and Shapley, 1976*a*) with a PDP 11/20 computer. We computed first and second harmonics of the modulation frequency in the response.

RESULTS

Rationale for Classification

The eel optic fibers were divided into classes on the basis of linearity of spatial summation. Understanding the rationale for this experimental procedure is essential for the interpretation of our results. The stimuli used for classifying the fibers were contrast reversal sine gratings. For each cell, gratings of several different spatial frequencies were used. Modulation was generally at 1 or 2 Hz. The space-averaged illuminance on the retina did not vary with time; rather, the spatial pattern was time modulated. The illuminance profile on the retina was $I_0 + I_1 \sin(2\pi kx + \phi) \sin(2\pi ft)$ where I_0 was the mean illuminance, I_1/I_0 was the contrast, k was spatial frequency, f was temporal frequency, and ϕ was spatial phase. The spatial phase (or position) dependence of the optic fiber's response to the contrast reversal grating determined whether we classed it as an X cell, or as an $\bar{X}$ cell, according to the following reasoning.

Suppose there were a single spatial mechanism in which light-evoked neural signals were added linearly. Then such a mechanism would have sensitivity for the contrast reversal grating which would be a sinusoidal function of the spatial phase of the grating (Hochstein and Shapley, 1976*a*). In particular, there would be two positions or spatial phases of the grating which evoke zero response. The same grating placed a quarter cycle away in either direction from one of these null positions (Enroth-Cugell and Robson, 1966) would give a maximum response for that grating. Furthermore, the responses of a linear spatial mechanism to a sinusoidally modulated grating would be sinusoidal in time, and these responses would be sinusoids at the modulation frequency only.

If the ganglion cell receives input from several spatial mechanisms within which and between which signals are pooled in a linear manner, and if these mechanisms produce responses which are in phase or exactly 180° out of phase with one another, then the ganglion cell will respond as if it received input from a single linear spatial mechanism. This equivalent single linear mechanism would be the algebraic sum of the several separate linear mechanisms. In particular, center and surround mechanisms which combine in a linear manner and produce responses exactly 180° out of phase with one another will be equivalent to a single linear spatial mechanism. Therefore, if a visual neuron does produce responses which vary in magnitude sinusoidally with the position of a contrast reversal sine grating, and if the responses of the cell are at the modulation frequency of the contrast reversal, one may conclude that the cell is being driven by a single linear spatial mechanism or its equivalent. Such a cell we call an X cell.

There are several different kinds of departures from the ideal linear case presented above. The first departure occurs when there are two (or more) linear mechanisms, but the responses from these separate mechanisms are not exactly in phase or exactly 180° out of phase with each other. This will occur if there are differences in the dynamics within the different mechanisms. In this case the responses of the neuron receiving these two (or more) inputs might not vary sinusoidally with spatial phase. In particular, there might be no null

positions. Nevertheless, the responses would be at the contrast modulation frequency. We have never observed this kind of departure from the ideal linear neuron in the eel retina.

An extreme example of a possible departure from the case of a single linear input is many nonlinear inputs. One particular model of this sort is a dispersed ensemble of small spatial subunits within which spatial pooling is linear but between which it is nonlinear. Such a model has been proposed to explain the behavior of Y cells in the cat retina (Hochstein and Shapley, 1976*b*). In this case, the response to a contrast reversal sine grating would be approximately constant with spatial phase—a marked departure from sinusoidal dependence on spatial phase. Furthermore, the responses would be mainly at the second harmonic of the modulation frequency, i.e. frequency-doubled or *on-off* responses.

It is possible to imagine receptive field models which are in some sense intermediate between the single linear mechanisms and the dispersed ensemble of nonlinear subunits. For instance, one might imagine a receptive field with one or only a few nonlinear subunits, or with many subunits which overlapped in one small retinal region. In this case, one would expect responses to be to some extent spatial phase dependent, but one would also expect responses to contain a large component at the second harmonic of the modulation frequency. This pattern of response is in fact what we have observed in about half of the eel optic fibers and such fibers have been tentatively labeled $\tilde{X}$. As will be seen below, the $\tilde{X}$ fibers were not like either X or Y ganglion cells of the cat retina.

Contrast Sensitivity

We will present most of the data in terms of the constrast sensitivity of the eel optic fibers. In general, nonlinearities after spatial summation can be avoided by using a sensitivity measure. Since sensitivity means the reciprocal of the stimulus required to achieve a fixed criterion response, nonlinearities in the stimulus-response relation of the output neuron do not affect sensitivity. Often we were able to work in a linear stimulus-response range, and thereby to make our sensitivity measurements equivalent to response measurements. In most fibers responses depended on contrast as shown in Fig. 1. They usually exhibited a substantial linear portion and then a soft saturation. Part of the reason we were able to work down in the linear range was technical. The microcomputer averager allowed measurement of small responses which might be at or near threshold for subjective measurement techniques.

An interesting number is the slope of the response vs. contrast curve in the linear range. This is a numerical specification of contrast sensitivity on an absolute scale in units of impulses/second ÷ contrast (cf. Hochstein and Shapley, 1976*a*). For the eel fibers of highest sensitivity this number was 300 imp/s ÷ contrast. Many eel ganglion cells were completely saturated by contrasts of 0.25–0.5.

Eel X Fibers

Out of 43 optic nerve fibers recorded in the eel, 21 were X-like. Responses from an eel X fiber are shown in Fig. 2. The stimulus was a contrast reversal

grating of 0.1 contrast, 2 Hz, and 1.3 cycles/mm on the retina. Three responses are shown. One is at the null position and the other two responses are at peak positions for the grating, a quarter-cycle away from the null position in either

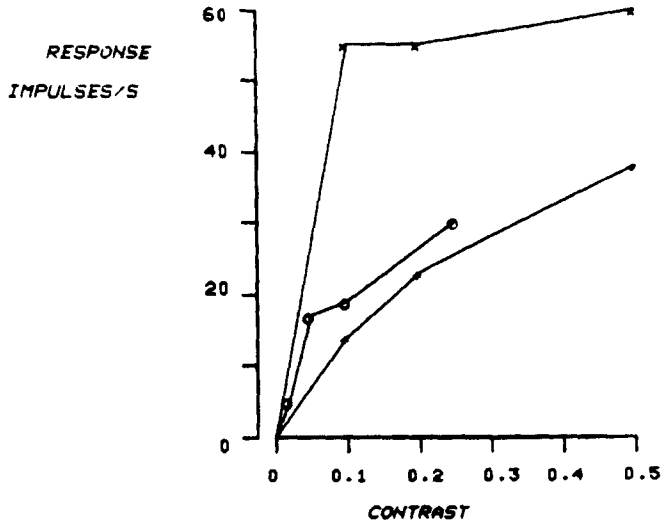

FIGURE 1. Response vs. contrast for X and $\bar{X}$ fibers. The fundamental amplitudes of the responses of an X cell to drifting gratings (1.3 cycles/mm; 2 Hz) are plotted as open circles. The peak response (at *off*) for an $\bar{X}$ fiber is plotted vs. contrast as x's. The secondary peak responses (at *on*) of the same $\bar{X}$ fiber are plotted as +'s. The $\bar{X}$ responses were to a contrast reversal grating (0.65 cycles/mm; 1 Hz).

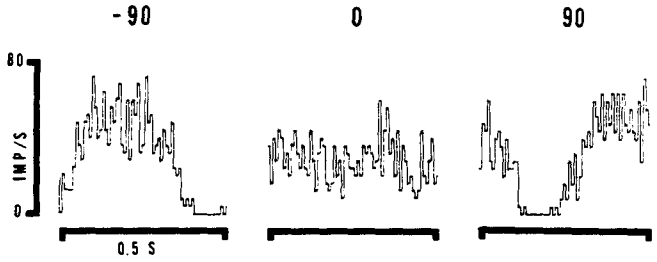

FIGURE 2. Eel X cell responses. The stimulus was a contrast reversal sine grating at 0.1 contrast, 2 Hz temporal modulation frequency, 1.3 cycles/mm spatial frequency. The spatial frequency was near the peak of this cell's spatial frequency sensitivity function. Spatial phase of the grating is written above each averaged response. At spatial phase zero, the grating was near the null position, and at ±90° spatial phase, the grating was eliciting a maximal response.

direction. The two peak positions were separated by 180° in spatial phase. The responses at the peak positions were mainly at the modulation frequency. This was confirmed by Fourier analysis of the responses.

For many X fibers, we measured responses at a number of spatial phases besides just at the peaks and nulls. The Fourier fundamental amplitude was calculated from the averaged responses. The sensitivity was derived from

responses at a number of contrasts as described above. Sensitivity in units of impulses/second ÷ contrast was plotted vs. spatial phase. Such a graph is shown in Fig. 3. It should be noted that, as in Fig. 2, responses on one side of a null were 180° out of phase with those on the other side of the null. In effect, the response changed sign. Therefore, we arbitrarily assigned a positive sign to one phase of response and a negative sign to the other phase of the response, and plotted them with this sign convention (cf. Hochstein and Shapley, 1976*a*). The second harmonic sensitivity was generally small in X fibers, and so we have not plotted it in Fig. 3. In Fig. 3, a smooth curve is plotted; this is the sine function which is the best fit to the points by the method of least squares. The

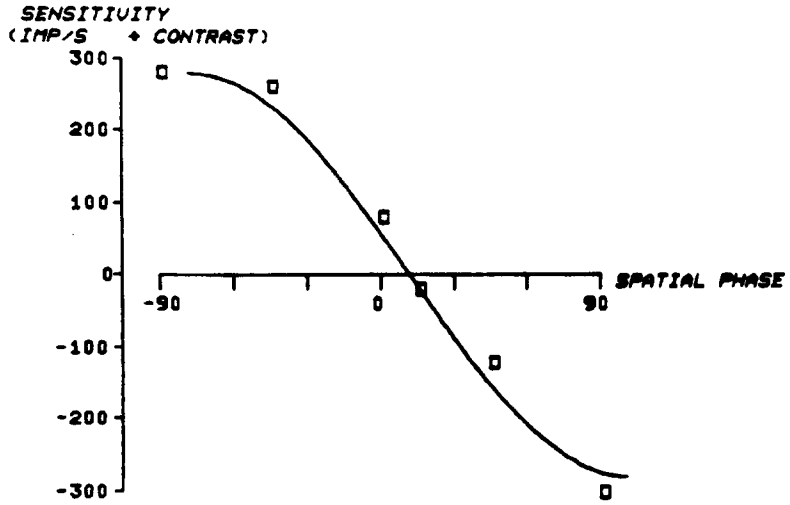

FIGURE 3. Sensitivity for the fundamental component of the response of an eel X cell as a function of spatial phase. The points □ are the fundamental amplitude of averaged responses like those in Fig. 1. The curve is a least-squares best fit sine wave. Points are plotted positive and negative because, in this cell, responses obtained at spatial phases >15° were 180° out of phase compared with responses to gratings with spatial phases <15°. This experiment was done with 1.3 cycles/mm and 2 Hz, spatial and temporal frequencies, respectively.

sensitivity of such a cell must be approximately a sinusoidal function of spatial phase, since the curve approximately fits the points.

Eel $\bar{X}$ Fibers

Some responses of an optic fiber which was not X-like are shown in Fig. 4. The two responses at the left-hand end and right-hand end of the figure are peak responses, and they were elicited by a contrast reversal grating at two positions 180° away from each other in spatial phase. The response in the middle was the minimum response which could be evoked by this contrast reversal grating, at a spatial phase 90° away from each of the peak positions. A plot of sensitivities for the first and second harmonic responses vs. spatial phase for another such fiber is shown in Fig. 5.

There was only a weak dependence of the fundamental response on spatial

phase. Therefore, in Fig. 5 the spatial phase axis is somewhat arbitrary. The second harmonic response in this type of fiber was much bigger in comparison with the first harmonic response than was the case with X fibers. From the pattern of responses in Fig. 4 and the presence of substantial second harmonic components in these responses, one might conclude that these eel ganglion cells were analogous to Y ganglion cells in the cat. However, this would be a mistake. Unlike cat Y cells, eel $\bar{X}$ cells produced a fundamental response amplitude with only a weak spatial phase dependence. Also, unlike the responses of true Y cells, the responses of $\bar{X}$ fibers did not become dominated by even harmonic components at high spatial frequencies. The second harmonic:first harmonic ratio did not become much greater than 1 at high spatial frequency. In Y cells of the cat retina, for example, this ratio may be above 10 when contrast reversal gratings of high spatial frequency are used as stimuli (cf. Hochstein and Shapley, 1976*a*). Other characteristics which distinguish $\bar{X}$ cells are described below.

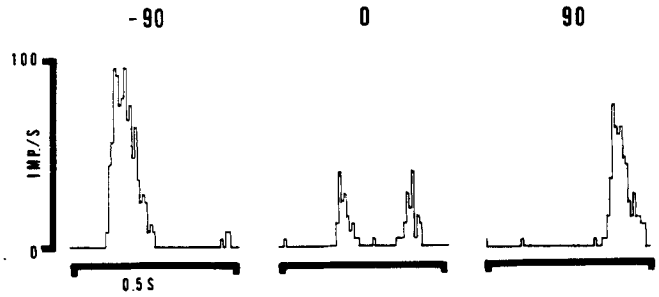

FIGURE 4. Responses to contrast reversal at different spatial phases for an $\bar{X}$ cell. Here the contrast reversal grating was modulated at contrast 0.3, at a rate of 2 Hz, and the grating had a spatial frequency of 0.65 cycles/mm. The spatial phase of 0° was the position at which the grating evoked the least response.

Most X and $\bar{X}$ fibers had zero or a very low mean rate in the absence of contrast modulation. There were two X fibers which were exceptional in having a mean rate exceeding 10 impulses/s. The $\bar{X}$ fibers had sensitivities comparable to the X fibers. Also, the dynamic range of their responses was not particularly compressed when compared with the X fibers. Thus there is no reason to view them as having sluggish responses to visual stimuli. It is important to note that the *on-off* responses in $\bar{X}$ fibers were approximately proportional to contrast. This is an important clue to the mechanism which underlies the frequency-doubled, or *on-off*, responses in these cells (see Discussion).

Responses to Drifting Gratings

Another stimulus was used to study the receptive field properties of eel optic fibers. This was the drifting sine grating. For this stimulus, the retinal illuminance was $I_0 + I_1 \sin \{2\pi(kx\text{-}wt)\}$ where I_0 was the mean illuminance, I_1/I_0 was contrast, k was spatial frequency in cycles/degree, and w was the temporal frequency in cycles/second. Usually, slow rates of drift between 0.5 and 2 cps were used.

Most eel X fibers behaved like their feline analogues in having a bandpass spatial frequency sensitivity. Several records from an X fiber in response to drifting gratings over a range of spatial frequencies are shown in Fig. 6. The

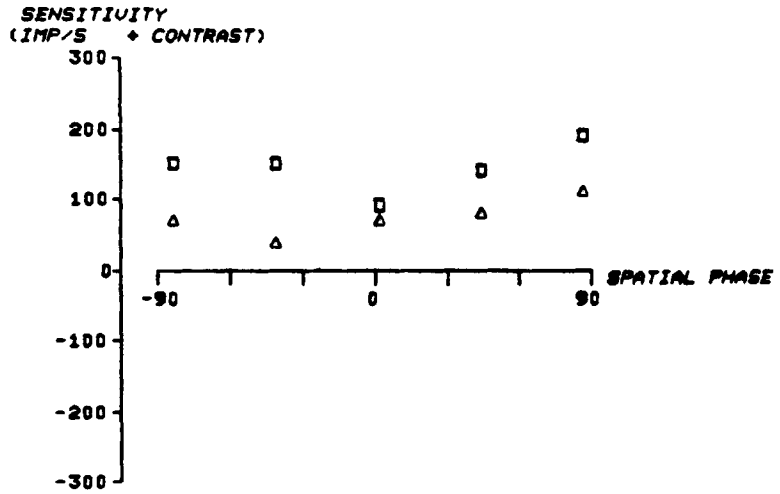

FIGURE 5. Sensitivity vs. spatial phase for an eel X̄ cell. The points marked □ are derived from the fundamental amplitudes, and the points marked with △ are from the amplitudes of the second harmonic response. The contrast reversal grating had a spatial frequency of 0.65 cycles/mm and a temporal frequency of 1 Hz. Amplitudes are plotted without sign, because the responses did not flip in phase by 180° when the grating was moved through the position of minimum sensitivity. There was no null position.

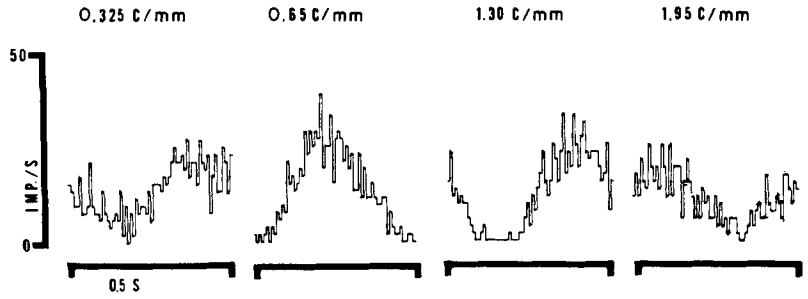

FIGURE 6. Responses of an X fiber to drifting gratings. This is a series of responses of an X fiber to drifting sine gratings at four different spatial frequencies but at a constant temporal frequency of 2 Hz. The spatial frequencies are marked above each record. The response was obtained by averaging 30 individual responses. There is a clear spatial tuning in this, as in most other eel X fibers, for spatial frequencies around 1 cycle/mm.

responses were mainly sinusoidal with a temporal frequency of response identical to the drift rate. The spatial frequency sensitivity function from two different X fibers is shown in Fig. 7. One X fiber had the usual bandpass spatial frequency sensitivity. The other type of X fiber had a low-pass spatial frequency sensitivity, and a rather low high-frequency cutoff for drifting

gratings. This was seen in several off-center X-like eel optic nerve fibers. The low spatial frequency cutoff of the spatial frequency sensitivity is associated with the presence of an antagonistic surround mechanism in the receptive field, and the high spatial frequency cutoff is determined by the resolving power of the receptive field center (cf. Enroth-Cugell and Robson, 1966). Thus the low-pass off-center X fibers presumably had large receptive-field centers and weak surrounds. This presumption was tested and verified by mapping the receptive field of the fiber with thin lines, as described below.

The $\bar{X}$ fibers almost always gave peculiar responses to drifting gratings. Some of these are illustrated for one such fiber in Fig. 8. At all spatial frequencies the response is complex, with large second harmonic and higher

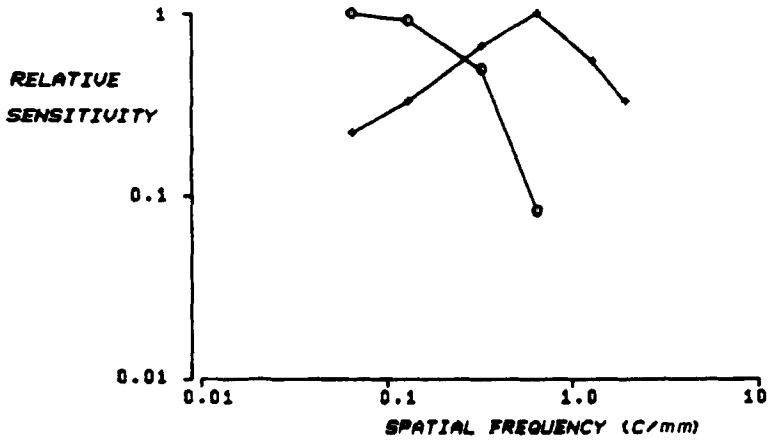

FIGURE 7. Spatial frequency sensitivity in eel X fibers. The spatial frequency sensitivity functions for two different types of eel X fiber are shown. O's are from a typical large off-center X fiber, while the small +'s are data from an on-center X cell with a strong antagonistic surround. The response measure used was fundamental Fourier amplitude, and sensitivity was derived from a series of responses at contrasts from 0.05 up to 0.25.

harmonic components (as determined by Fourier analysis of the response). It appears that for gratings of low spatial frequency, the $\bar{X}$ fiber gives an *on-off* response to each of the bars of the drifting grating. Such behavior is never observed in cat Y cells, but it has been described for some W cells in the cat retina (Cleland and Levick, 1974) and for what seem to be analogous cells in the rabbit retina (Levick, 1967). This complex behavior can be accounted for by a fairly simple receptive field model which we will present in the Discussion. The model implies that the peculiar behavior of the eel $\bar{X}$ fibers when they are driven by drifting gratings is not inconsistent with their pattern of response to contrast reversal gratings.

It was possible to construct spatial frequency responses for $\bar{X}$ fibers, although the interpretation of these curves was not so straightforward as it was in the case of X fibers. The spatial frequency response of two representative $\bar{X}$ fibers is shown in Fig. 9. Usually, these were low-pass responses and the spatial resolution was not as good as for the high-resolution X cells.

From the spatial frequency resolution of eel optic fibers one can infer the effective summing area of the receptive field center. Our results imply that eel X fibers summate over an area of ~0.3 mm². The smallest summing area we found in X fibers was 0.1 mm². $\tilde{X}$ fibers sum light-evoked signals over a larger area – ~0.6 mm².

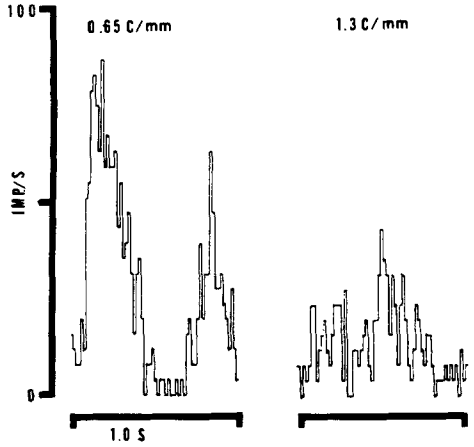

FIGURE 8. Responses of an $\tilde{X}$ fiber to drifting sine gratings. These responses were obtained at a drift rate of 1 Hz and a contrast of 0.1. There is a very evident two-peaked response at the lower spatial frequency, a characteristic of $\tilde{X}$ fibers.

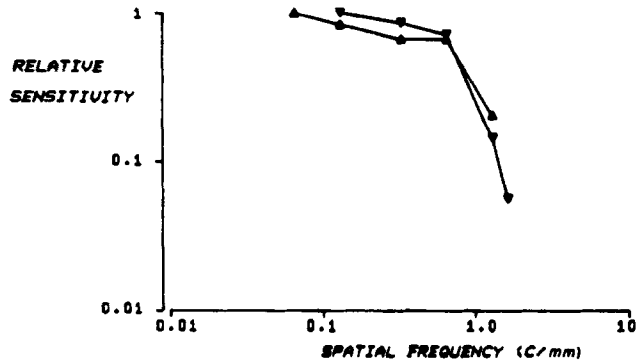

FIGURE 9. Spatial frequency sensitivity for $\tilde{X}$ fibers. These data were obtained at a drift rate of 1 Hz (▽) and 2 Hz (△) on two different $\tilde{X}$ fibers. The absence of a low-frequency rolloff is characteristic. The response measure used was peak response in 30 ms. Sensitivity was calculated from a series of responses at different contrasts.

The temporal frequency resolution of the eel ganglion cells was poor at the background which was used (0.2 lm/m²). Typically, there was no audible impulse rate modulation for temporal modulation exceeding 4 Hz. This suggests that the ganglion cells were driven mainly by a rod pathway.

Line Weighting Functions

On many of the eel optic fibers we mapped the spatial sensitivity distribution in

one or two dimensions by measuring the sensitivity as a function of position for a thin bar modulated in intensity. The illuminance of the bar was $I_0 + I_1 \sin 2\pi wt$, and its width was in the range of 0.3–0.6 mm. Line-weighting functions were obtained on fewer cells than were studied with contrast reversal or drifting gratings. Yet the results obtained were consistent between fiber types, and were also consistent enough with the grating data to give some confidence that the conclusions from line-weighting experiments were reliable.

The typical X fiber had a strong surround antagonistic to the receptive field center. A line-weighting function for such a cell is shown in Fig. 10. Once we encountered an X fiber with an asymmetrical line-weighting function as shown in Fig. 11. Such a fiber would be more sensitive to luminance borders than to any other stimulus.

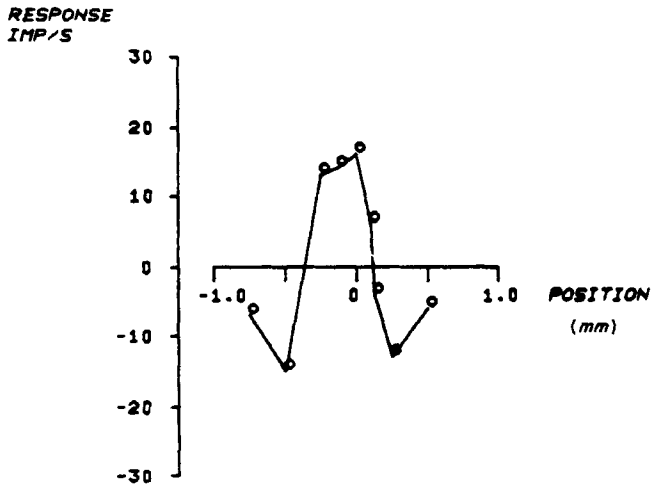

FIGURE 10. Response profile for an X fiber. Fundamental Fourier amplitude is plotted vs. position of a 0.3-mm bar in the receptive field of the fiber. The bar was modulated plus and minus around the steady background with a sinusoidal temporal waveform at 1 Hz. Contrast was 0.25.

The typical $\bar{X}$ fibers gave local *on-off* responses to thin lines presented in their receptive fields. The line-weighting function of one particular $\bar{X}$ fiber is shown in Fig. 12. In this graph the sensitivity to local increase of illumination (*on* response) is plotted separately from the sensitivity to a local decrease of illumination (*off* response). Note particularly that the *on* and *off* profiles have peaks with roughly similar widths at half-height. Also note the wide tail for the *on* response. Other treatments of the data are possible, but we intend to argue in the Discussion that this segregation of *on* and *off* response in $\bar{X}$ fibers may lead to some insight. Often in $\bar{X}$ fibers the *on* and *off* sensitivity profiles were not concentric.

Radial Symmetry

Most eel X optic fibers possessed radial symmetry but there were exceptions. The asymmetric X cell mentioned above (cf. Fig. 11) had an orientational

preference, for example. In another case, we found an X cell with a radially symmetric center but an elliptical antagonistic surround mechanism. This was deduced from spatial frequency responses taken at right angles in orientation. The high-frequency cutoffs were the same at the two orientations, but the low-frequency attenuation (presumably due to the surround) was somewhat weaker in one orientation than in the other.

DISCUSSION

The finding of X and $\bar{X}$ cells in the retina of a fish reinforces the idea that diversity of retinal ganglion cells is a general property of vertebrate retinas. The eel ganglion cells fall into clear classes which are distinguished by the

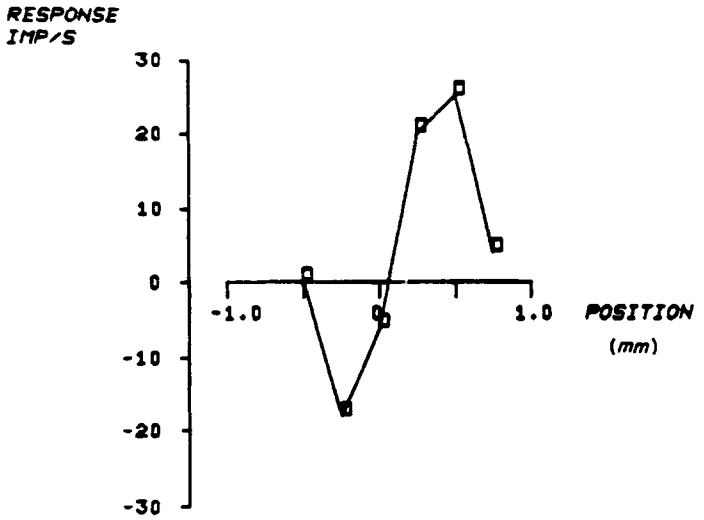

FIGURE 11. Response profile for an asymmetric X fiber. The contrast was 0.5 and the bar width was 0.6 mm. Here the response measure was peak impluse rate (in 30 ms). Temporal modulation frequency was 1 Hz.

fundamental criterion that they sum light-evoked signals in completely different ways. Many X fibers resemble the X ganglion cells of the cat retina. They sum light-evoked signals in a linear manner, have relatively small receptive fields, and respond better to a grating of an optimal spatial frequency than they do to diffuse light or coarse gratings. Other eel X cells, the large-field, off-center cells, are unlike any cells which have been studied in the cat.

The $\bar{X}$ ganglion cells of the eel retina are unlike cat Y cells in that they do not give a spatial phase-insensitive, frequency-doubled response to fine gratings. Many of their receptive-field properties resemble those described for one of the subclasses of W ganglion cells in the cat retina—the class called local edge detectors, or *on-off* cells (Cleland and Levick, 1974; Stone and Fukuda, 1974). For instance, they produce an *on-off* response to local stimulation (Fukuda and Stone, 1974; Cleland and Levick, 1974) and frequency-doubled responses to drifting gratings (Cleland and Levick, 1974). The eel cells differ from the *on-off* W cells of the cat retina in that they respond to diffuse light.

Receptive Field Models

It is useful to formulate models for the spatial mechanisms which produce the responses of retinal ganglion cells. To the extent that a model accounts for experimental observations, it is a concise explanation of underlying mechanisms. To disprove or to confirm a model is a challenge for future experiments.

The linear model of Rodieck (1965) has provided insight into the working of X ganglion cells in the cat retina (cf. Enroth-Cugell and Robson, 1966). The great resemblance of eel X cells to cat X cells implies that the Rodieck model ought to be considered as an explanation of the receptive-field properties of eel X cells. Just to summarize the Rodieck model, it consists of two overlapping spatial mechanisms (called center and surround) which produce responses of opposite sign. Local responses within each mechanism are added up in a linear

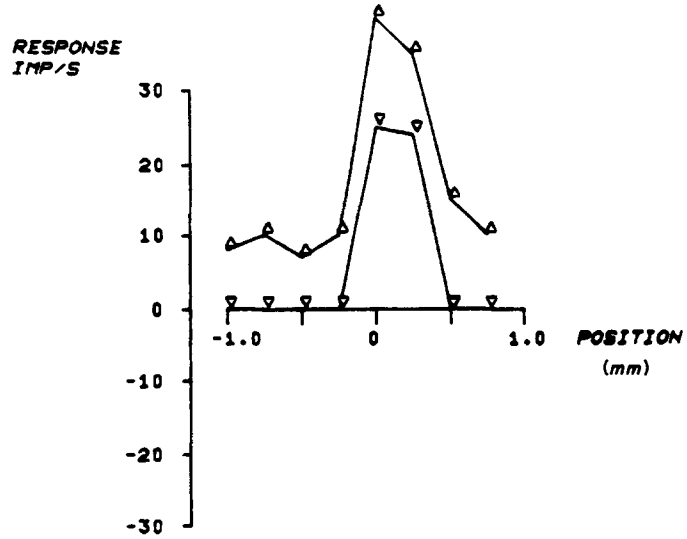

FIGURE 12. Response profile for an $\bar{X}$ fiber. The *off* response is plotted as ∇ and the *on* response as Δ. The *on*-response mechanism was more sensitive and had a wider "tail" than did the *off* mechanism. Modulation frequency was 1 Hz and contrast was 0.25. The bar width was 0.5 mm. Note that the two mechanisms are not peaking in quite the same spot.

way, and then the pooled center signal is added to the pooled surround signal. Eel X cells give linear local responses; they produce spatial phase-sensitive responses to contrast reversal gratings; and they respond best to some optimal spatial frequency. These three crucial results are consistent with a Rodieck-type model for eel X cells.

The $\bar{X}$ cells produce responses which cannot be explained in terms of the Rodieck model. However, it is possible to formulate a model which does account for most of the $\bar{X}$ behavior, and resembles the Rodieck model in having only two spatial mechanisms. The contrast sensitivity profiles of the two mechanisms in the $\bar{X}$ model are drawn in Fig. 13. It is clear that these two mechanisms are roughly comparable in size, unlike the center and surround

mechanisms in the Rodieck model. The two mechanisms are not concentric. Furthermore, one must postulate some kind of nonlinearity to account for the nonlinear character of $\tilde{X}$ responses to local stimulation and to gratings. We postulate that within each spatial mechanism pooling is linear. However, the pooled output of each mechanism must pass through the physiological equivalent of a half-wave rectifier. Perhaps this element is a rectifying synapse (cf. Hochstein and Shapley, 1976*b*). One of these two mechanisms is excited by increments, and so might be called the *on* response mechanism. The other is the *off* mechanism. Since the responses of these mechanisms are rectified, they are not mutually antagonistic. The *off* mechanism cannot cancel the response to the *on* mechanism and vice versa. The idea of two independent mechanisms for *on* and *off* responses in *on-off* cells is consistent with the recent work of Levine and Shefner (1977).

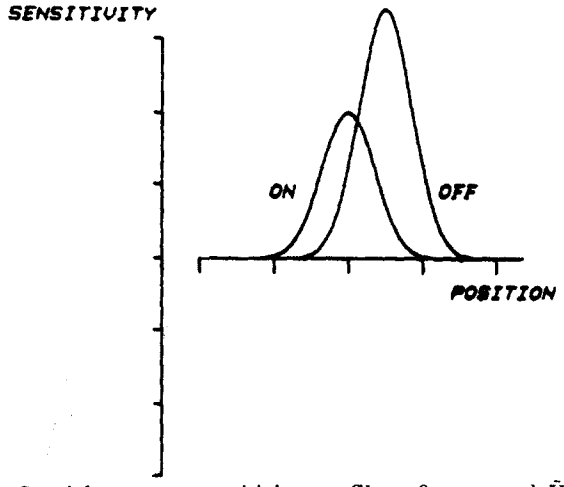

FIGURE 13. Spatial contrast-sensitivity profiles of proposed $\tilde{X}$ model. It is proposed that there are two overlapping spatial mechanisms which pool linearly within their own summation areas, but between which there is a rectifying nonlinearity. These two mechanisms are assumed to be opposite in sign. It is assumed that their midpoints are somewhat displaced from each other. In different cells, the relative strengths of these *on* and *off* mechanisms are probably different.

The response of this model to contrast reversal gratings is like that of the $\tilde{X}$ cells. It will show spatial phase sensitivity, but no null position (because the *on* and *off* mechanisms are not concentric). Even at high spatial frequency it will retain spatial phase sensitivity; in this respect it is unlike the multisubunit model of Y cells formulated by Hochstein and Shapley (1976*b*). To local stimulation or to diffuse light, the $\tilde{X}$ cell model will generate *on-off* responses. Because the nonlinearity is rectification, the nonlinear responses of the model will grow in proportion to the contrast or depth of modulation, as is observed in $\tilde{X}$ cells (Fig. 1). Also, the responses of this model to drifting gratings of low spatial frequency will exhibit *on-off* responses to the bars of the grating, as is indeed observed in $\tilde{X}$ cells. Both qualitatively and quantitatively, this nonlinear model with two rectifying subunits appears to explain the behavior of $\tilde{X}$ cells.

Further experiments will probably require embellishment of the model for $\bar{X}$ cells. For example, we have not explored the effects of changes in background illuminance on the properties of $\bar{X}$ cells. It is likely that the receptive field properties of $\bar{X}$ cells do depend on mean illuminance, and so will the properties of a more complete model. However, we feel that the model in Fig. 13 accounts for the essential features of these cells at the scotopic background we used.

A nonlinear model with two rectifying subunits also may be adequate to explain the behavior of *on-off* retinal ganglion cells in other species. Unfortunately, no experimental data exist on spatial summation in the responses to contrast reversal gratings in cat *on-off* W cells. However, judging from the responses to local stimulation, diffuse light, and drifting gratings (Stone and Fukuda, 1974; Cleland and Levick, 1974), we would infer that a somewhat modified model of the type presented in Fig. 13 might suffice to account for *on-off* W cell responses. The modification which is required is the introduction of a center-surround organization within the two subunits. This modification is required because of the poor responses of the *on-off* cat W cells to diffuse light.

Evolutionary Considerations

This is an initial investigation of retinal ganglion cells in a cold-blooded vertebrate by means of contemporary techniques of receptive field analysis. What it has demonstrated is that there are striking similarities between types of ganglion cells in a fish retina and some of the types of ganglion cells one finds in a mammalian retina. Although there are probably special classes of cell present in the eel retina and not in the mammal, and vice versa, nevertheless the great majority of ganglion cells recorded in the eel have a mammalian analogue. Furthermore, the quality of vision provided to the eel by his retinal ganglion cells is in some ways not distinctly inferior to that provided to, say, a cat by his ganglion cells. The contrast sensitivity of eel ganglion cells falls well within the mammalian range. The presence of spatial tuning is similar in eel and cat ganglion cells.

However, the spatial resolution of eel ganglion cells is considerably poorer than that of the cat when considered in terms of cutoff frequencies in cycles per millimeter. The cat ganglion cells with the best acuity can resolve 25 cycles/mm, i.e., 5 cycles/deg where 1 deg ≡ 0.2 mm in a cat. The best resolution in eel X-like ganglion cells was around 2.5 cycles/mm. However, it is possible that we somehow might have missed fibers with a higher spatial resolution in the eel. The eel's spatial resolution is even poorer when considered in terms of cycles per degree of visual angle because the eel's eye is so small—approximately 5 mm in diameter. One can calculate that each degree of visual angle corresponds to about 80 μm in the eel. Therefore, the highest-resolution eel ganglion cells resolved only about $^1/_{30}$th as well as the highest-resolution cat cells. This probably is adequate for the watery world the eels inhabit, a world in which high acuity vision is probably not beneficial. It is a curious fact that the resolution of ommatidia in the eye of the horseshoe crab is comparable to the best eel X cells, at about 0.16 cycles/deg (S. Brodie, personal communication). Perhaps evolutionary pressures in the sea force marine animals to develop eyes with only low spatial resolution.

There is the further question of the evolutionary continuity of the X cells

from fish to mammals. The central connections of X and $\bar{X}$ cells in eels are not known. In cats, the X optic fibers project only to the lateral geniculate nucleus and not to the superior colliculus (Hoffman and Stone, 1973). It would be interesting to know if the X fibers in the eel project to the optic tectum, the structure homologous to the mammalian superior colliculus. If they do, their central projection would differ from that seen in cats. Perhaps the connection between X fibers and colliculus, forbidden in cats, is not so forbidden in other vertebrates.

This work was supported in part by grants EY 1472, EY 188, and EY 1428 from the United States National Eye Institute. Computer time was provided in part by the C.U.N.Y. Computer Center.

Received for publication 10 June 1977.

REFERENCES

CLELAND, B. G., and W. R. LEVICK. 1974. Properties of rarely encountered types of ganglion cells in the cat's retina and an overall classification. *J. Physiol. (Lond.).* **240**:457–492.

ENROTH-Cugell, C., and J. G. ROBSON. 1966. The contrast sensitivity of the retinal ganglion cells of the cat. *J. Physiol. (Lond.).* **187**:517–552.

FUKUDA, Y., and J. STONE. 1974. Retinal distribution and central projections of Y-, X-, and W-cells of the cat's retina. *J. Neurophysiol.* **37**:749–772.

HARTLINE, H. K. 1938. The response of single optic nerve fibers in the vertebrate eye to illumination of the retina. *Am. J. Physiol.* **121**:400–415.

HOCHSTEIN, S., and R. M. SHAPLEY. 1976*a*. Quantitative analysis of retinal ganglion cell classifications. *J. Physiol. (Lond.).* **262**:237–264.

HOCHSTEIN, S., and R. M. SHAPLEY. 1976*b*. Linear and nonlinear spatial subunits in Y cat retinal ganglion cells. *J. Physiol. (Lond.).* **262**:265–284.

HOFFMAN, K. P., and J. STONE. 1973. Central terminations of W-, X-, and Y-type ganglion cells from cat retina. *Brain Res.* **49**:500–501.

KUFFLER, S. W. 1953. Discharge patterns and functional organization of mammalian retina. *J. Neurophysiol.* **16**:37–68.

LEVICK, W. R. 1967. Receptive fields and trigger features of ganglion cells in the visual streak of the rabbit's retina. *J. Physiol. (Lond.).* **188**:285–307.

LEVINE, M. W., and J. M. SHEFNER. 1977. Variability in ganglion cell firing patterns; implications for separate "ON" and "OFF" processes. *Vision Res.* **17**:765–776.

MATURANA, H. R., J. Y. LETTVIN, W. S. McCulloch, and W. H. PITTS. 1960. Anatomy and physiology of vision in the frog *Rana pipiens*. *J. Gen. Physiol.* **43** (Suppl.):125–175.

MILKMAN, N., R. M. SHAPLEY, and G. SCHICK. 1978. A Microcomputer-Based Visual Stimulator. Behavior Research Methods & Instrumentation. In press.

Rodieck, R. W. 1965. Quantitative analysis of cat retinal ganglion cell response to visual stimuli. *Vision Res.* **5**:583–610.

RODIECK, R. W. 1973. The Vertebrate Retina. W. H. Freeman & Co., San Francisco, Calif.

SHAPLEY, R. M., and M. ROSSETTO. 1976. An electronic visual stimulator. *Behav. Res. Methods Instrum.* **8**:15–20.

STONE, J., and Y. FUKUDA. 1974. Properties of cat retinal ganglion cells: a comparison of W-cells with X- and Y-cells. *J. Neurophysiol.* **37**:722–748.